Par-VSOM: Parallel and Stochastic Self-organizing Map Training Algorithm

Omar X. Rivera-Morales and Lutz Hamel
Department of Computer Science, University of Rhode Island, College Road, South Kingstown, Rhode Island, U.S.A.

Keywords: SOM, VSOM, GPU, Parallel Computing, Self-organizing Map, Stochastic Training, Vector Optimization.

Abstract: This work proposes Par-VSOM, a novel parallel version of VSOM, a very efficient implementation of stochastic training for self-organizing maps inspired by ideas from tensor algebra. The new algorithm is implemented using parallel kernels on GPU accelerators. It provides performance increases over the original VSOM algorithm, PyTorch Quicksom parallel version, Tensorflow Xpysom parallel variant, as well as Kohonen's classic iterative implementation. Here we develop the algorithm in some detail and then demonstrate its performance on several real-world datasets. We also demonstrate that our new algorithm does not sacrifice map quality for speed using the convergence index quality assessment.

1 INTRODUCTION

The self-organizing map (SOM) is a neural network designed for unsupervised machine learning (Kohonen, 2001). The generated maps are powerful data analysis tools applied to diverse areas such as atmospheric science, nuclear physics, pattern recognition, medical diagnosis, computer vision and other data domains (Barney, 2018; Li et al., 2018a; Ramos et al., 2017). See reference (Kohonen, 2001) for a more comprehensive literature survey. Here we introduce the Parallel VSOM (Par-VSOM), a parallel implementation of the efficient VSOM algorithm (Hamel, 2019). The novel approach presented here, replaces all iterative constructs of the SOM algorithm with kernels running in a hardware accelerator to perform vector and matrix operations in parallel. The algorithm kernels provide substantial performance increases over Kohonen's SOM iterative algorithm, the *XpySom*(Mancini et al., 2020), and *Quicksom* (Mallet et al., 2021b; Mallet et al., 2021a) parallel BatchSOM implementations.

The training of the SOM is computationally demanding, but a great advantage of SOMs is that the computations can be parallelize with algorithm modifications like in the BatchSOM or using hardware vectorization. Currently, various types of hardware accelerators are easily available, allowing us to process Big-Data (Morán et al., 2020) datasets using high-performance computers (HPC), Graphical Processing Units (GPU), and Field Programmable Gate Arrays (FPGA)(Richardson and Winer, 2015; Abadi et al., 2016).This research provides an alternative efficient SOM algorithm to accelerate the training of highly complex rectangular maps.

Our experiments demonstrate that our parallel algorithm is better suited for highly computational demanding maps, such as the maps generated with large SOMs. Using a large number of neurons provides a higher resolution clustering of the data and facilitates the pattern recognition during the analysis, as shown in Figure 1. Furthermore, the maps produced by the Par-VSOM are equivalent in quality to the maps produced by the original SOM iterative algorithm. The current Par-VSOM model is parallel and multi-threaded, and therefore well suited as a replacement for other parallel algorithms to train the self-organizing maps.

The paper is organized as follows: In Section 2, we start our discussion with an overview of the SOM and a brief introduction to the VSOM (Hamel, 2019) vectorized rules, which can be viewed as an implementation of a competitive learning scheme comprised of a competitive step and an update step with vector and matrix training. The relevant details about related research work are included in Section 3. As part of Section 4, we develop the Par-VSOM vector-based parallel training and examine the data level parallelisms achievable using vectorized single instruction with multiple data (SIMD) registers and discuss the limitations. Under Section 5, we included the study of the performance of our parallel vectorized

Rivera-Morales, O. and Hamel, L.
Par-VSOM: Parallel and Stochastic Self-organizing Map Training Algorithm.
DOI: 10.5220/0011377700003332
In *Proceedings of the 14th International Joint Conference on Computational Intelligence (IJCCI 2022)*, pages 339-348
ISBN: 978-989-758-611-8; ISSN: 2184-3236

training implementation by comparing it to various CPU and GPU SOMs variants. Finally, in Section 6, we conclude our discussion with a summary of the observations and some future research ideas under consideration.

2 THE SOM AND VSOM ALGORITHMS

The origins of the self-organizing maps model can be traced back to the Vector Quantization (VQ) method (Kohonen, 2001). The VQ is a signal-approximation algorithm that approximates a finite "codebook" of vectors $m_i \in R^n, i = 1,2,...,k$ to the distribution of the input data vector $x \in R^n$. In the SOM context, the approximated codebook allows us to categorize the nodes and forms an "elastic network," which becomes a meaningful, coordinated map or grid system.

From a computational perspective, the SOM can be described as a mapping of high dimensional input data onto a low dimensional neural network projected as a 2D or three-dimensional (3D) constrained topological map (Hastie et al., 2001). The mapping is accomplished by assuming that the input data set is a real vector such as $x_k = [\xi_1, \xi_2, ..., \xi_n]^T \in R^n$. The SOM neuronal map can be defined as a model containing the parametric real vector $m_i = [u_{i1}, u_{i2}, ..., u_{in}]^T \in R^n$ associated with the neurons' weights. If we consider the distance between the input vector x_k and the neuron vector m_i then we can establish an initial minimum distance relation between the input and the neurons by calculating the Euclidean distances. Then, these distances are used to identify the best matching unit (BMU) index with equation (1).

$$c = \underset{i}{\operatorname{argmin}}(||\mathbf{m}_i - \mathbf{x}_k||^2) \tag{1}$$

To define the SOM in terms of matrix and vector operations it is assumed that the map's neurons are stored in a $n \times d$ matrix $\mathbf{M}$ where each row i represents the neuron $\mathbf{m}_i$ with d components,

$$\mathbf{M}[i,] = \mathbf{m}_i = (m_1, \ldots, m_d)_i, \tag{2}$$

with $i = 1, \ldots, n$. The training data x consists of a set D= $\{\mathbf{x}_1, \ldots, \mathbf{x}_l\}$. The set can be defined as a $l \times d$ matrix where each row k represents the training vector $\mathbf{x}_k$ with d components,

$$\mathbf{D}[k,] = \mathbf{x}_k = (x_1, \ldots, x_d)_k, \tag{3}$$

with $k = 1, \ldots, l$.

Essential details to consider include (1) the dimensionality d for the input, and (2) the neuron vectors

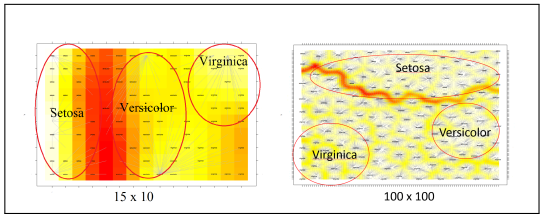

Figure 1: IRIS 15x10 small SOM and IRIS 100x100 large SOM, neuronal heatmaps patterns with different resolutions.

are required to be the same size for well-defined matrix operations.

2.1 The SOM and VSOM Competitive Step

In the competitive step, we find the BMU for a particular training instance $\mathbf{x}_k$. In the classic SOM we use an iterative process to find the BMU using 1. Here the $i = 1,2,...,n$ represents the index of the neurons in the map and $\mathbf{m}_i$ represents the neuron in index i. The *argmin* is a function that returns the minimum value and c contains the index of the BMU.

In the VSOM context this step requires us to calculate the Euclidean distance as a set of vector and matrix operations. These operations find the c index associated with the neuron with the minimum distance to the training instance. The BMU c index corresponds to the neuron in the map with the highest resemblance to the particular $\mathbf{x}_k$ selected for training during the epoch.

The first step to calculate the BMU requires us to compute a matrix X to hold a randomly selected training vector. The matrix X in equation (4) is defined with a component sizes of $n \times d$, where each row is holding the current epoch *training vector* $\mathbf{x}_k = (x_1, x_2, \ldots, x_d)_k$, which is randomly selected from matrix $\mathbf{D}$,

$$\mathbf{X} = \mathbf{1}^n \otimes \mathbf{x}_k. \tag{4}$$

Here, the symbol $\otimes$ represents the outer product and $\mathbf{1}^n$ is a column vector defined as,

$$\mathbf{1}^n = \underbrace{(1,1,\ldots,1)}_{n}^{\mathbf{T}}. \tag{5}$$

Since $\mathbf{1}^n$ is a column vector and $\mathbf{x}_k$ is a row vector the operation in (4) is well defined. After populating the instance matrix X with the duplicated $\mathbf{x}_k$ values, equations (6), (7) and (8) are used to compute the square of the Euclidean distances between all the map neurons and the selected input vector,

$$\Delta = \mathbf{M} - \mathbf{X} \tag{6}$$

$$\Pi = \Delta \circ \Delta \tag{7}$$

$$\mathbf{s} = \Pi \times \mathbf{1}^d \tag{8}$$

In equation (6) we calculate the difference between the matrices with an element-by-element matrix subtraction. In equation (7) we use the Hadamard product to allow us to calculate the Π matrix, in this context $\circ$ represents the element-by-element matrix product and X, M, Δ and Π are all $n \times d$ matrices.

Lastly, in equation (8) we use a 'row sum' matrix reduction to compute the vector $\mathbf{s}$ of size n. Here, $\mathbf{1}^d$ is a column vector similar to (5) with the dimensionality defined by the value of d.

2.2 The SOM and VSOM Update Step

In the classic stochastic SOM, after completing the BMU calculations, the updates to the neuronal weights are accomplished using the training instance x_k to influence the best matching neuron and its surrounding neighborhood.

$$\mathbf{m}_i \leftarrow \mathbf{m}_i - \eta(\mathbf{m}_i - \mathbf{x}_k)h(c,i) \tag{9}$$

The weights update step in equation (9), affects every neuron inside the neighborhood radius of influence. Here, the learning rate η serves as a scaling factor between 0 and 1. The $h(c,i)$ acts as the loss function , where i = 0, 1, ... , n and it can be defined as,

$$h(c,i) = \begin{cases} 1 & \text{if } i \in \Gamma(c), \\ 0 & \text{otherwise,} \end{cases} \tag{10}$$

where $\Gamma(c)$ is the neighborhood of the best matching neuron $\mathbf{m}_c$ with $c \in \Gamma(c)$. In the classic SOM, the learning factor and the loss function both decreased monotonically over time (Kohonen, 2001).

In the VSOM, the update step for all the neurons in the map is accomplished with matrix operations and is defined as,

$$\mathbf{M} \leftarrow \mathbf{M} - \eta\Delta \circ \Gamma_c. \tag{11}$$

Here, η is the learning rate, Δ contains the calculations of the difference between the neurons and the selected training instance as computed in (6), and the symbol $\circ$ represents the Hadamard product. The Hadamard product represent by $\circ$ is the element-by-element matrix product. Similarly to the SOM, in the VSOM, the learning rate η is linearly reduced as epochs increase.

However, our experimental results demonstrate that a constant learning rate η generates higher quality convergence indexes in large map instances. Initially, the update rule for each best matching neuron has a very large radius of influence and includes all the neurons on the map. After multiple training epochs, the neighborhood radius around the BMU gradually shrinks to the point that the field of influence only includes the best matching neuron $\mathbf{m}_c$ as shown in (12).

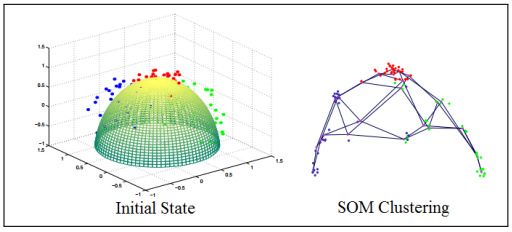

Figure 2: SOM preserving the neighborhood topology in 3D space (Hastie et al., 2001).

$$\Gamma(c)|_{t \gg 0} = \{c\}. \tag{12}$$

The competitive and the update steps are computed during each epoch using the randomly selected training instances until some convergence criterion is fulfilled. After reaching a maximum convergence, every data point will be assigned to an specific data neuron forming clusters in the grid and preserving the neighborhood topology as shown in Figure 2.

Algorithm 1 and 2 summarizes the matrix and vector operations required for the parallel Par-VSOM training. For a more detailed explanation of the SOM and VSOM algorithms, see reference (Hamel, 2019).

3 RELATED WORK

In this section, we look at prior work related to parallel SOM algorithms and its applications. Recent parallel self-organizing maps research has demonstrated promising improvements using various parallel methods. Some of the methodology mentioned in current scientific publications on this topic include: combining data and network partitioning techniques (Richardson and Winer, 2015; Silva and Marques, 2007), exploiting cache effects (Rauber and Merkl, 2000), using map-reduce programming paradigm (Sarazin et al., 2014; Sul and Tovchigrechko, 2011; Schabauer and Weishaupl, 2005), replacing the SOM iterative construct with vector and matrix operations (Hamel, 2019), and using various types of accelerated architectures for parallelism (Davidson, 2015; Moraes et al., 2012; Abadi et al., 2016; Mancini et al., 2020; Wittek et al., 2013). In addition, recent publications demonstrate how to utilize SOM as a pattern recognition tool (Kim et al., 2020; Li et al., 2018b; Lokesh et al., 2019). In general, recent research publications share similars goals such as: finding new applications, improving optimal performance and increasing speed-up using different SOM approaches.

3.1 SOM Parallel Hybrid Methods

The combination of data and network partitioned parallel methods develop by Richarson et al. (Richardson and Winer, 2015) splits up the map to compute the best matching calculation and nodes update on separate threads. This hybrid methodology also divides the data amongst individual threads for data partition parallelism. As part of their research findings, they concluded that parallelizing the classic SOM algorithm using such techniques in a GPU can save computation time and increase the speed-up by nearly 15X in maps with 10,000 points and 5 dimensions. A similar method was proposed by (Silva and Marques, 2007), achieving a performance increases of 1.27X training large maps on a small HPC cluster.

3.2 SOM Vectorization

The VSOM by (Hamel, 2019) replaced all the iterative constructs of the standard stochastic SOM algorithm with vector and matrices operations. The VSOM implementation resulted in a performance increase of up to 60X faster after running 10000 iterations in a 25 X 20 map. Since the VSOM seems to be offering the highest speed-up increase of all the current SOM research publications, our research is focus on the parallelization of the VSOM algorithm and its implementation in hardware accelerators.

3.3 SOM in Multiple Parallel Architectures

Among the SOM parallel approaches previously discussed, not many offer an available open source repository to validate the research findings or continue with further investigations. In this paper, we decided to compare our proposed parallel implementation with some of the widely available parallel SOM projects packages. As part of the GPU comparisons we utilize, *Quicksom* (Mallet et al., 2021a) which offers a parallel GPU Batch-SOM algorithm implemented using the Python PyTorch framework and speed-ups results showed at least a 20 speed-up over the CPU version using bioinformatics datasets (Mallet et al., 2021b). In addition, we also included a comparison with *XpySom* (Mancini et al., 2020) a parallel Batch-SOM variant implemented using the Google Tensorflow 2.0 framework and Python Numpy library. The *XpySom* package is based on the Minisom(Vettigli, 2021), a non-parallel, minimalistic and Numpy based widely know implementation of the SOM. The *XpySom* research paper (Mancini et al., 2020) indicates their parallel variants outperforms the popular SOM GPU package *Somoclu* by two and three orders of magnitude.

4 Par-VSOM: PARALLEL VECTORIZED SOM

4.1 Hardware for Parallel Vectorization

Our novel parallel implementation is based on the VSOM algorithm proposed by (Hamel, 2019). On the VSOM, the stochastic SOM training is redefined to execute as a set of vector and matrix operations. Since all the matrix data elements are independent of each other, they can be executed as coarse-grained "embarrasingly parallel" tasks to exploit multiple hardware threads (or cores) available in the devices (Jaaskelainen, 2019). In the VSOM context, the vectorization of the calculations can be implemented as vector instructions, which are also known as SIMD instructions and are a form of Data-Level Parallelism. These vector instructions apply the same operation over multiple data elements (like integers and floating-point values) concurrently, given that these items are stored contiguously in vector/SIMD registers (Pilla, 2018). In modern Intel and AMD CPU architectures, these vector instructions are known as Advance Vector Extensions (AVX), AVX2, AVX-512 instructions set and Streaming SIMD Extensions (SSE4).

In contrast, the GPUs with their substantial amount of nodes allows for the creation of thousands of threads to perform vector calculations simultaneously. Furthermore, the current NVIDIA GPUs can access there memory much faster when accessing adjacent data concurrently. This is optimized when groups of 32 GPU threads or warps do the request simultaneously, causing "memory coalescing" (Dickson et al., 2011).

4.2 Par-VSOM Algorithm

In the classic SOM with iterative operations, the operations per column are solved in a loop structure sequentially. This serial approach results in high overhead and additional latency during every training epoch. Conversely, the VSOM vector and matrix operations are vectorized by the compiler, and they are executed in the CPU as vector operations. To illustrate, in a data set with 32 instances, the VSOM using vectorized operations will need to execute a total of four "*minus*" operations to compute a Δ matrix entirely. Using the VSOM vectorization, the Δ matrix "*minus*" operation can be completed with a speed-up

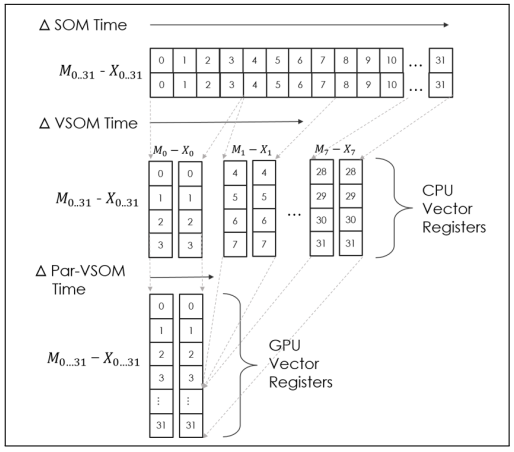

Figure 3: The time comparison of Δ calculation during the competitive step for SOM, VSOM, and PAR-VSOM demonstrate modern architecture advances in vectorization capability increases the primitive operations' overall speed-up performance.

increase of 4X compared to the SOM, as illustrated in Figure 3.

In the Par-VSOM, the vector and matrix operations of the original VSOM are replaced with parallel computational kernels executing in a hardware accelerator architecture. The parallel kernels manipulate the matrices columns in a unified vector V_u as shown in equation (13). In the kernel, the matrices are expressed as tuples of column vectors and encapsulated into one unifying vector. Based on the data of our example in Figure 3, the unifying vector technique will result in executing the 32 elements operation in one single vectorized operation, providing a performance increase of 128x.

$$\mathbf{V_u}[i*n] = (t_1,\ldots,t_n)_1 \cup (t_1,\ldots,t_n)_2 \ldots \cup (t_1,\ldots,t_n)_i \quad (13)$$

In the unifying vector equation (13), we have shown how the matrices can be express in terms of union of tuples. Here, $\cup$ represents the union operator. In the Par-SOM algorithm (1) and (2), we are assuming all the matrices of the VSOM are implemented as a data structure consisting of multiple tuples $(t_1,t_2,...,t_n)$ where each column is represented by the tuple $(t_n)_i$ with i representing the dimensionality of the matrix and n the number of instances. This technique allows the data-level parallelism to occur by executing all the matrix operations as optimized vector operations inside the Φ kernels as presented in algorithm 1 and 2.

In our GPU implementation, we decided to use CUDA Thrust. Considering that the Par-VSOM is a parallel and vectorized implementation of the VSOM algorithm, the Thrust template is an ideal candidate due to the vast number of vector functions available. In addition, Thrust manages all the CUDA kernel initialization, memory transfers and allocation in the background, and provides highly optimized libraries for vector operations (Nvidia.com, 2020).

Algorithm 1: The Par-VSOM training algorithm.

Given:
D $\leftarrow$ {training instances, a l x d matrix}
M $\leftarrow$ {neurons, a n x d vector of tuples}
$\eta \leftarrow$ {learning rate $0 < \eta < 1$}
$\Gamma(c) \leftarrow$ {neighborhood function for some neuron c}
minIndex(s) $\leftarrow$ {returns location of min. val in s}
$\Phi \leftarrow$ {Vectorized kernel operation, with all matrices columns unified as tuples in a single column vector.}

Repeat
/***Select a matrix training instance as vector for some $k = 1,...,l$ and $f = 1,...,d$: ***/
$x_k \leftarrow \mathrm{D}[k][1] \cup \mathrm{D}[k][2] ... \cup \mathrm{D}[k][f]$
/***Find the winning neuron using kernels ***/
$\mathrm{X} \leftarrow \Phi_x(1^n \otimes x_k)$
$\Delta \leftarrow \Phi_\Delta(\mathrm{M} - \mathrm{X})$
$\Pi \leftarrow \Phi_\Pi(\Delta \circ \Delta)$
/***Sum of vector subsections (rowsum) ***/
$s \leftarrow \Phi_s(\Pi_{1...(n*1)} + \Pi_{(n*1)...(n*2)} + \ldots \Pi_{(n*(d-1)...(n*d)})$
c = minIndex(s)
/***Update neighborhood with vector operations ***/
$\Gamma_c \leftarrow \Phi_\Gamma(\Gamma(c))$
$M_{new} \leftarrow \Phi_{M_{new}}(M_{current} - \eta\Delta \circ \Gamma_c)$
Until done
return $\mathbf{M_{new}}$

Algorithm 2: The Par-VSOM Neighborhood Function $\Gamma(c)$ as mentioned in equation (10) and (11).

Given:
$c \leftarrow$ {index of winning neuron}
$n \leftarrow$ {the number of neurons on the map}
nsize $\leftarrow$ {neighborhood radius}
$\mathbf{P} \leftarrow$ {an $n \times 2$ vector with $\mathbf{p}_i = \mathbf{P}[i,] = (x_i, y_i)$}
$\mathbf{1}^n \leftarrow$ {constant column vector with value 1}
$\mathbf{0}^n \leftarrow$ {constant column vector with value 0}
$\Phi \leftarrow$ Vectorized kernel operation, with all matrices columns unified as tuples in a single column vector.
$\mathbf{x} \leftarrow$ { x values in first section: 1,...,$(\frac{n}{2} - 1)$}
$\mathbf{y} \leftarrow$ { y values in second section: $\frac{n}{2}, ..., (n \times 2)$}
$P_c \leftarrow \Phi_{pc}(P[c,])$
$\mathbf{C} \leftarrow \Phi_C(\mathbf{1}^n \otimes \mathbf{p}_c)$
$\Delta \leftarrow \Phi_\Delta(\mathbf{P} - \mathbf{C})$
$\Pi \leftarrow \Phi_\Pi(\Delta \circ \Delta)$
/***Perform rowsum with vector subsections
$\mathbf{d} \leftarrow \Phi_d(\Pi_x + \Pi_y)$
hood $\leftarrow \Phi_{hood}(\text{ifelse}(\mathbf{d} < (nsize \times 1.5)^2, \mathbf{1}^n, \mathbf{0}^n))$
return hood

Since most of the VSOM algorithm consists of matrix operations, we utilized Thrust specialized transformation and reduction functions to process the matrices as vectors. In the case of a matrix with three columns, storing 3d points as an array of float3 in CUDA is generally a bad idea, since array accesses are not properly coalesced (Nvidia.com, 2020). To address this memory access issue, the number of rows n was used as a delimiter to identify the beginning and the end of each column in the unifying vector Vu. The column-wise encapsulation of the matrix transforms the three-dimensional columns in to one Vu vector. This allows coalesced memory access and faster operation execution.

One of the important differences between the original VSOM algorithm and the Par-VSOM algorithm , is the data structure manipulation during the selection of the D matrix random training instance algorithm 1 (line 13). Here, the training computation transforms the selection into an X_k vector that includes all the matrix D columns and allows us to find the BMU using vector operations. To be able to use the optimized "minIndex(s)" function in line 22, we reduced the Π vector with length $n*d$ into a vector of length n, using operations equivalent to a rowsum across d dimensions in line 20.

Similarly, the Par-VSOM neighborhood Function Γ in algorithm 2, emulates the rowsum operations of algorithm 1 in line 18 by utilizing the vector elements representing the x and y columns accordingly and returns one vector that includes the distances of the neurons in the grid. In lines 19 to 20 using the computed distances, the vector neighborhood determination is performed and return a **hood** vector that activates the neurons considered to be part of the neighborhood by flipping to "1" their corresponding neurons index.

4.3 Limitations

4.3.1 Large Computational Workloads

The Par-VSOM is recommended for clustering problems requiring high computational workloads. To obtain our experimental results, we tested with multiple datasets and various map sizes. The results demonstrated the Par-VSOM is not suitable for small maps, low-dimensional datasets, or minimal computational workloads. Here, we assume the users will have a GPU hardware accelerator available as part of their setup.

In general, Big data and other extensive datasets analysis requires generating large neuronal maps as part of the pattern analysis and clusters visualizations. The GPUs have become one of the default tools to process high complexity problems and are easily accessible in cloud environments, but we are aware that not everyone may have access to one.

5 EXPERIMENTS

5.1 Hardware Setup

All the Par-VSOM, *Xpysom* and *Quicksom* parallel experiments were performed using the Amazon AWS cloud service instances with Linux and Deep Learning Amazon Machine Images (AMI). The sequential CPU experimental setting included an Intel I7-7700K running at 4.20 GHz/ 4.50GHz turbo with four cores and capable of executing eight threads. The GPU tests were performed in an AWS P3.2xlarge with 18 virtual Intel Xeon E5 2686 CPU operating at 2.7 GHz/ 3.0 GHz turbo and an NVIDIA Tesla V100. The Tesla V100 contains 5120 NVIDIA Cuda cores with 16 Gb of HBM2 memory. The Tesla V100 memory clock setting was 877 Mhz with memory graphics clocked at 1530 Mhz.

5.2 Par-VSOM Setup and Hyper-parameters

The experimental setup utilized the default values of the SOM and VSOM *Popsom* (Hamel et al., 2016). For the *Quicksom*(Mallet et al., 2021b) and *Xpysom*(Mancini et al., 2020) BatchSOM packages, we maintained the learning rate constant to obtain higher convergence indexes and tune the hyper-parameters as defined in Table 1.

Table 1: Par-VSOM Hyper-Parameters.

Hyper-Parameters	**Values**
Training Iterations	1×10^0 ... 1×10^5
Learning Rate η	0.7
Neighborhood Radius	Bubble, Gaussian(for *Quicksom*)
Map sizes	15x10, 150x100, 200x150
Datasets	Iris, Epil, WDBC

As part of our tests, we compared the performance and the quality of the maps generated by our parallel Par-VSOM with two CPU SOM and two GPU SOM variants. The quality of the maps is based on the convergence index as define in (Tatoian, 2018). The CPU single-node tests used the SOM and the VSOM algorithms included as part of the R language *Popsom* package with C bindings applications. In contrast, the parallel comparisons were done using the two GPU-based SOM packages; *Quicksom* with Python 3, Pytorch 1.4 and *Xpysom* using Tensorflow 2.0 in their

Table 2: Times and Speed-up gains of the Par-VSOM for different training algorithms using a 200×150 map.

iter	Time SOM(s) CPU R\C	Time VSOM(s) CPU R\Fortran	Time P-VSOM(s) GPU Cuda Thrust	Time Xpysom(s) CPU-GPU TensorFlow	Time Quicksom(s) CPU-GPU PyTorch	Speed-up Par-VSOM/ SOM	Speed-up Par-VSOM/ VSOM	Speed-up Par-VSOM/ Xpysom	Speed-up Par-VSOM/ Quicksom
*** Iris D=4***									
1	1.148	0.035	0.027	0.301	0.257	42.5	1.3	11.1	9.5
10	1.350	0.046	0.029	0.319	0.257	46.6	1.6	11.0	8.9
100	2.362	0.067	0.049	0.414	0.434	48.2	1.4	8.4	8.9
1000	13.447	0.324	0.235	1.408	2.32	57.2	1.4	6.0	9.9
10000	124.011	2.756	1.925	10.742	21.456	64.4	1.4	5.6	11.1
100000	1228.811	26.210	18.275	110.900	212.791	67.2	1.4	6.1	11.6
*** Epil D=8***									
1	1.831	0.053	0.046	0.300	0.262	39.8	1.2	6.5	5.7
10	1.949	0.058	0.049	0.313	0.259	39.8	1.2	6.9	5.3
100	3.125	0.108	0.072	0.412	0.643	43.4	1.5	5.7	8.9
1000	14.854	0.554	0.294	1.411	4.667	50.5	1.9	4.8	15.8
10000	132.193	4.928	2.577	10.660	46.755	51.3	1.9	4.1	18.1
100000	1306.793	47.560	22.535	115.372	462.908	58.0	2.1	5.1	20.5
*** WDBC D=30***									
1	0.966	0.152	0.125	0.303	0.262	7.7	1.2	2.4	2.0
10	1.167	0.165	0.130	0.319	0.256	9.0	1.3	2.5	2.0
100	3.161	0.342	0.174	0.416	0.762	18.2	2.0	2.5	4.4
1000	23.236	2.076	0.601	1.387	6.386	38.7	3.5	2.3	10.6
10000	222.034	19.105	4.712	11.389	63.871	47.1	4.1	2.4	13.6
100000	2224.134	188.080	46.114	111.223	634.687	48.2	4.1	2.4	13.8

Table 3: Quality of maps produced by the different training algorithms (SOM=Classic SOM, VSM=VSOM, P-V=Par-VSOM, X-P=Xpysom, Q-S=Quicksom and D=Dimensions).

iter	15x10					150x100					200x150				
10^x	SOM	VSM	P-V	X-P	Q-S	SOM	VSM	P-V	X-P	Q-S	SOM	VSM	P-V	X-P	Q-S
*** Iris, D=4***															
1	0.50	0.15	0.09	0.50	0.45	0.41	0.00	0.00	0.50	0.12	0.40	0.00	0.00	0.50	0.08
2	0.43	0.53	0.48	0.37	0.49	0.02	0.45	0.49	0.50	0.50	0.34	0.45	0.49	0.47	0.50
3	0.92	0.95	0.93	0.88	0.48	0.42	0.79	0.49	0.40	0.50	0.12	0.85	0.77	0.32	0.50
4	0.93	0.91	0.91	0.92	0.37	0.92	0.91	0.96	0.28	0.48	0.92	0.93	0.91	0.29	0.48
5	0.95	0.94	0.94	0.87	0.27	0.96	0.99	0.95	0.26	0.41	0.90	0.99	0.97	0.32	0.37
*** Epil, D=8***															
1	0.03	0.14	0.15	0.72	0.40	0.12	0.00	0.00	0.46	0.06	0.12	0.00	0.0	0.46	0.13
2	0.70	0.56	0.40	0.60	0.48	0.03	0.45	0.45	0.49	0.50	0.07	0.38	0.40	0.50	0.50
3	0.92	0.92	0.94	0.81	0.80	0.31	0.68	0.53	0.36	0.50	0.27	0.40	0.64	0.41	0.50
4	0.94	0.92	0.93	0.65	0.79	0.45	0.48	0.68	0.29	0.86	0.85	0.60	0.56	0.40	0.56
5	0.96	0.91	0.93	0.95	0.78	0.85	0.97	0.96	0.40	0.84	0.91	0.98	0.93	0.38	0.54
*** WDBC, D=30***															
1	0.31	0.14	0.11	0.68	0.37	0.00	0.00	0.00	0.62	0.13	0.07	0.00	0.00	0.50	0.00
2	0.50	0.53	0.50	0.67	0.66	0.08	0.51	0.45	0.53	0.55	0.27	0.55	0.44	0.50	0.50
3	0.90	0.92	0.88	0.50	0.80	0.30	0.48	0.64	0.40	0.66	0.40	0.60	0.63	0.40	0.50
4	0.92	0.90	0.90	0.69	0.67	0.47	0.81	0.80	0.43	0.89	0.52	0.85	0.85	0.44	0.50
5	0.89	0.92	0.93	0.68	0.68	0.88	0.90	0.91	0.37	0.76	0.81	0.97	0.98	0.37	0.50

implementation.

For our experiments we used three real-world datasets to train our algorithms:

1. Iris (Fisher, 1936) - a dataset with 150 instances and 4 attributes that describes three different species of Iris.
2. Epil (Thall and Vail, 1990) - a dataset on two-week seizure counts for 59 epileptics. The data consists of 236 observations with 8 attributes. The dataset has two classes - placebo and progabide, a drug for epilepsy treatment.
3. Wisconsin Breast Cancer Dataset (wdbc) (Street et al., 1993) - a dataset with 30 features and 569 instances related to breast cancer in Wisconsin, for our experiment we generated a random normalized sample of 100 instances. The dataset has two classes: malignant and benign.

These datasets are purposely selected to test the algorithm performance by increasing the dimensionality complexity of the input data. To measure the Par-VSOM performance, we ran each timing test three times and took the average time over these runs. The times reported are the time required for the CPU to perform the calculations and it is given in CPU seconds. Similarly, the quality tests were done by averaging three quality measurements using the convergence index (CI) explain in detail in (Tatoian, 2018) and included as part of the R *Popsom* Package (Hamel et al., 2016). The CI provides a 0 to 1 numbering scale to measure the maps' quality, with 0 represents the

lowest quality and 1 the highest quality. Furthermore, three map sizes were considered for these experiments, 15×10 (small), 150×100 (medium), 200×150 (large), to see how the different implementations perform on different map sizes. In addition, we trained with various number of training iterations (in powers of 10) to discover what type of effect a change of training duration had on the implementations.

5.3 Results

In the large map environment results included in Table 2, we see the recurrent speed-up gains of the algorithm with larger maps. The large size of data buffers require for the calculations, the CPU cache memory size limitations and DDR4 lower clock rate does present an performance impact for the SOM and VSOM CPU variants. The large workload and substantial computational resources available in the GPU, allows the Par-VSOM performance scale further. Here, the Par-VSOM achieves a speed-up of 67 in comparison to the SOM. The table results demonstrates, the Par-VSOM achieves superior speed-up in all the three datasets comparisons, surpassing the speed rates of all the other algorithm implementations. In this large map environment, the Par-VSOM surpassed the SOM with a 67, the VSOM with a 4.1, *Xpysom* with 6.1 and the *Quicksom* by 20 speed-up increase.

The training time charts included in Figure 4, capture a generalize representation of the overall results. The Par-VSOM offers speedup performance increases for the three datasets in medium and larger size maps instances. The obtained results allows us to establish a direct relation between large neuronal maps and better achievable times using the Par-VSOM. That is, with a higher number of neurons an scalable speed up can be achieved.

The Table 3 illustrates the baseline quality of original algorithms using our three datasets. The results present us with a recurring behaviour in most of the maps, their is a pattern to decrease the convergence quality when the datasets dimensionality increases. However, we also identified as the size of the maps increases, there is tendency for the vectorized variants (VSOM and Par-VSOM) to generate higher quality maps. Furthermore, our testing demonstrates *Xpysom* and *Quicksom* SOM parallel versions can not reach a high convergence index when larger map sizes are used.

In terms of the quality of the maps, Figure 5 captures all the algorithm convergence indexes for the three datasets. As illustrated, the Par-VSOM maintains relatively the same quality as the original SOM

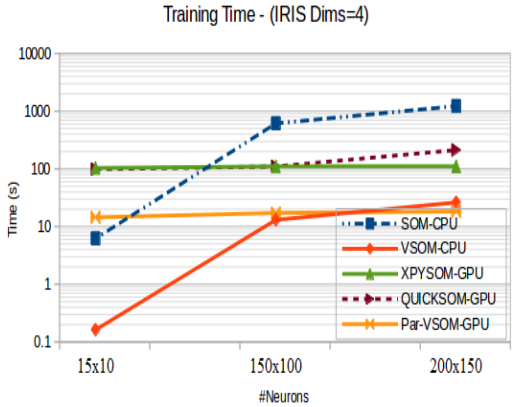

(a) Iris Total Training Time at Convergence

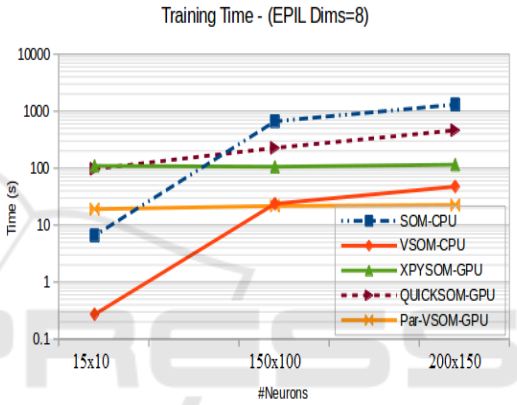

(b) Epil Total Training Time at Convergence

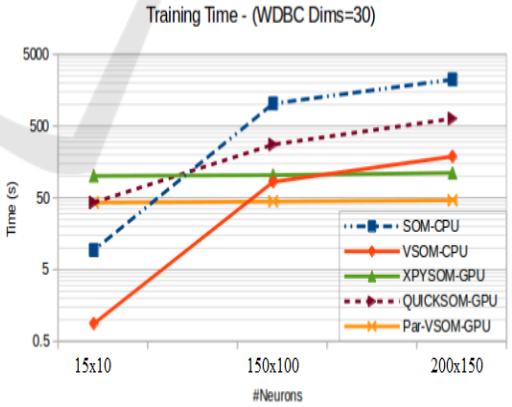

(c) WDBC Total Training Time at Convergence

Figure 4: Total training time for all datasets with multiple map sizes at the convergence iteration 100000.

and the VSOM variants in all the maps. In contrast, the parallel GPU BatchSOM variants (*Xpysom* and *Quicksom*) only obtained good quality indexes with smaller maps (15 x 10). In both of these parallel packages, the convergence index quality starts decreas-

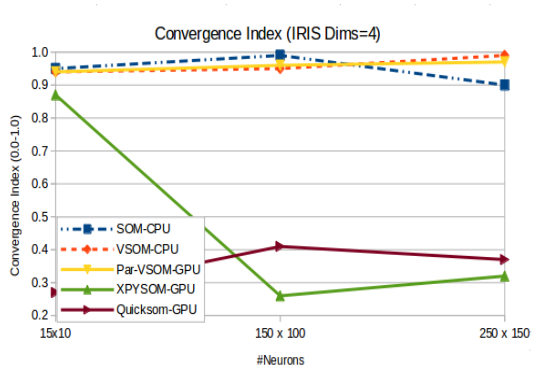

(a) Iris Convergence Index (Map Quality)

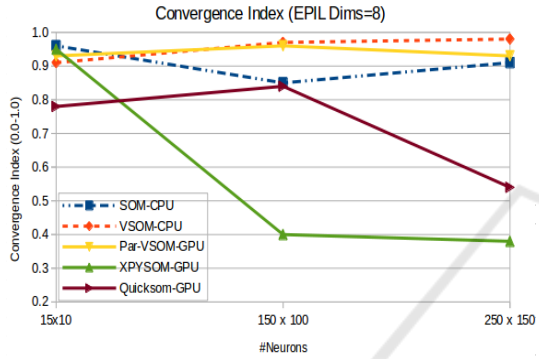

(b) Epil Convergence Index (Map Quality)

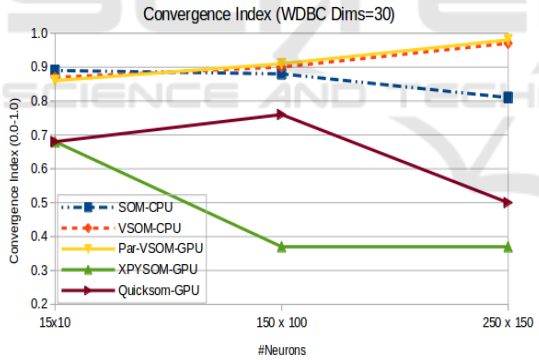

(c) WDBC Convergence Index (Map Quality)

Figure 5: Convergence Index for the three datasets with various map sizes.

ing drastically after trying to organized medium and larger SOM maps.

6 CONCLUSIONS

This work introduced the Par-VSOM, a highly parallel, vectorized and matrix-based implementation of stochastic training for self-organizing maps. The novel implementation presented here provides substantial performance increases over Kohonen's iterative SOM algorithm (up to 67 times faster), the CPU based vectorized VSOM (up to 4 times faster), the GPU *Xpysom* (up to 6.1 times) and *Quicksom's* GPU (up to 20 times) in large maps environments. The results clearly indicate the parallel BatchSOM approach provided by *Xpysom* and *Quicksom's* are no longer the most optimal parallel option in newer architectures due to the overhead and latency added by search for winner in the batch algorithm. The performance gains follow a direct relation with the increment of the map sizes, as shown in Figure 4. Furthermore, the results obtained by increasing the dimensionality and maps sizes demonstrated the Par-VSOM provides a scalable speed-up performance when the neuronal map size increases. In terms of the quality of the maps, the maps produced by Par-VSOM approximates the high quality values generated by the VSOM iterative algorithms and original Kohonen's SOM algorithm.

In the proposed design, the Par-VSOM is a multithreaded algorithm running in a GPU and therefore is an adequate replacement for iterative stochastic training of SOM and parallel SOM variants. We are currently investigating how the Par-VSOM can be implemented in an FPGA and what kind of performance increase we can expect from this type of hardware architecture. Based on our results, the Par-VSOM can be viewed as an alternative to parallel SOM and a new alternative for other parallel algorithms for clustering and pattern recognition. In summary, since the training algorithms results demonstrate the produce maps are roughly the same quality, the Par-VSOM provides a parallel and high-performance alternative to SOM algorithms. The Par-VSOM source code is available at (Rivera-Morales, 2022).

REFERENCES

Abadi, M., Jovanovic, S., Ben Khalifa, K., Weber, S., and Bedoui, M. (2016). A scalable flexible som noc-based hardware architecture. *Advances in Self-Organizing Maps and Learning Vector Quantization*, pages 164–175.

Barney, B. (2018). *Introduction to Parallel Computing*. Lawrence Livermore National Laboratory.

Davidson, G. (2015). A parallel implementation of the self organising map using opencl. *University of Glasgow*.

Dickson, N. G., Karimi, K., and Hamze, F. (2011). Importance of explicit vectorization for cpu and gpu software performance. *Journal of Computational Physics*, 230(13):5383–5398.

Fisher, R. A. (1936). The use of multiple measurements in taxonomic problems. *Annals of eugenics*, 7(2):179–188.

Hamel, L. (2019). Vsom efficient, stochastic self-organizing map training. In *Proceedings of the 2018 Intelligent Systems Conference (IntelliSys) Volume 2*, pages 805–821.

Hamel, L., Ott, B., and Breard, G. (2016). *popsom: Functions for Constructing and Evaluating Self-Organizing Maps*. R package version 4.1.0.

Hastie, T., Tibshirani, R., and Friedman, J. (2001). *The Elements of Statistical Learning*. Springer Series in Statistics. Springer New York Inc., New York, NY, USA.

Jaaskelainen, P. (2019). Task parallelism with opencl: A case study. *Journal of Signal Processing Systems*, pages 33–46.

Kim, K.-H., Yun, S.-T., Yu, S., Choi, B.-Y., Kim, M.-J., and Lee, K.-J. (2020). Geochemical pattern recognitions of deep thermal groundwater in south korea using self-organizing map: Identified pathways of geochemical reaction and mixing. *Journal of Hydrology*, 589:125202.

Kohonen, T. (2001). *Self-organizing maps*. Springer Berlin.

Li, J., Chen, B. M., and Lee, G. H. (2018a). So-net: Self-organizing network for point cloud analysis. In *Proceedings of the IEEE conference on computer vision and pattern recognition*, pages 9397–9406.

Li, T., Sun, G., Yang, C., Liang, K., Ma, S., and Huang, L. (2018b). Using self-organizing map for coastal water quality classification: Towards a better understanding of patterns and processes. *Science of The Total Environment*, 628-629:1446–1459.

Lokesh, S., Kumar, P. M., Devi, M. R., Parthasarathy, P., and Gokulnath, C. (2019). An automatic tamil speech recognition system by using bidirectional recurrent neural network with self-organizing map. *Neural Computing and Applications*, 31(5):1521–1531.

Mallet, V., Nilges, M., and Bouvier, G. (2021a). Quicksom. https://github.com/bougui505/quicksom.

Mallet, V., Nilges, M., and Bouvier, G. (2021b). quicksom: Self-organizing maps on gpus for clustering of molecular dynamics trajectories. *Bioinformatics*, 37(14):2064–2065.

Mancini, R., Ritacco, A., Lanciano, G., and Cucinotta, T. (2020). Xpysom: high-performance self-organizing maps. In *2020 IEEE 32nd International Symposium on Computer Architecture and High Performance Computing (SBAC-PAD)*, pages 209–216. IEEE.

Moraes, F. C., Botelho, S. C., Duarte Filho, N., and Gaya, J. F. O. (2012). Parallel high dimensional self organizing maps using cuda. In *2012 Brazilian Robotics Symposium and Latin American Robotics Symposium*, pages 302–306. IEEE.

Morán, A., Rosselló, J. L., Roca, M., and Canals, V. (2020). Soc kohonen maps based on stochastic computing. In *2020 International Joint Conference on Neural Networks (IJCNN)*, pages 1–7.

Nvidia.com (2020). Thrust quick start guide. https://docs.nvidia.com/cuda/thrust/index.html#abstract. Accessed: 2020-04-30.

Pilla, L. L. (2018). Basics of vectorization for fortran applications. *Research Report*, RR-9147:1–9.

Ramos, M. A. C., Leme, B. C. C., de Almeida, L. F., Bizarria, F. C. P., and Bizarria, J. W. P. (2017). Clustering wear particle using computer vision and self-organizing maps. In *2017 17th International Conference on Control, Automation and Systems (ICCAS)*, pages 4–8.

Rauber, Andreas, P. T. and Merkl, D. (2000). parsom: a parallel implementation of the self-organizing map exploiting cache efects: making the som fit for interactive high-performance data analysis. In *Proceedings of the IEEE-INNS-ENNS International Joint Conference on Neural Networks. IJCNN 2000*, volume 6.

Richardson, T. and Winer, E. (2015). Extending parallelization of the self-organizing map by combining data and network partitioned methods. *Advances in Engineering Software*, 88:1–7.

Rivera-Morales, O. (2022). Par-vsom. https://github.com/oxrm/Par-vsom.

Sarazin, T., Azzag, H., and Lebbah, M. (2014). Som clustering using spark-mapreduce. In *2014 IEEE International Parallel & Distributed Processing Symposium Workshops*, pages 1727–1734. IEEE.

Schabauer, Hannes, E. S. and Weishaupl, T. (2005). Solving very large traveling salesman problems by som parallelization on cluster architectures. In *Sixth Internatioanl Conference on Parallel and Distributed Computer Applications and Technologies PDCAT' 05*, pages 954–958. IEEE.

Silva, B. and Marques, N. (2007). A hybrid parallel som algorithm for large maps in data-mining. *New Trends in Artificial Intelligence*.

Street, W. N., Wolberg, W. H., and Mangasarian, O. L. (1993). Nuclear feature extraction for breast tumor diagnosis. In *IS&T/SPIE's Symposium on Electronic Imaging: Science and Technology*, pages 861–870. International Society for Optics and Photonics.

Sul, S.-J. and Tovchigrechko, A. (2011). Parallelizing blast and som algorithms with mapreduce-mpi library. In *2011 IEEE International Symposium on Parallel and Distributed Processing Workshops and Phd Forum*, pages 481–489. IEEE.

Tatoian, R.and Hamel, L. (2018). Self-organizing map convergence. *International Journal of Service Science, Management, Engineering, and Technology (IJSSMET)*, 9(2):61–84.

Thall, P. F. and Vail, S. C. (1990). Some covariance models for longitudinal count data with overdispersion. *Biometrics*, pages 657–671.

Vettigli, G. (2021). Minisom. https://github.com/JustGlowing/minisom.

Wittek, P., Gao, S. C., Lim, I. S., and Zhao, L. (2013). Somoclu: An efficient parallel library for self-organizing maps. *arXiv preprint arXiv:1305.1422*.